Forest Ecology and Management 454 (2019) 117659

Contents lists available at ScienceDirect

Forest Ecology and Management

journal homepage: www.elsevier.com/locate/foreco

First-entry wildfires can create opening and tree clump patterns characteristic of resilient forests

Van R. Kane[a,*], Bryce N. Bartl-Geller[a], Malcom P. North[b], Jonathan T. Kane[a], Jamie M. Lydersen[c], Sean M.A. Jeronimo[a], Brandon M. Collins[d], L. Monika Moskal[a]

[a] School of Environmental and Forest Sciences, University of Washington, Seattle, WA 98195, USA
[b] USDA Forest Service, PSW Research Station, Mammoth Lakes, CA 93546, USA
[c] California Department of Forestry and Fire Protection, Fire and Resource Assessment Program, Sacramento, CA 95818, USA
[d] University of California Berkeley, Berkeley, CA 94720, USA

ARTICLE INFO

Keywords:
ICO
Forests
Frequent fire
Reference areas
Resilience
Tree clumps
Openings
Tall trees
Burn severity
Lidar

ABSTRACT

A century of fire suppression has left fire-dependent forests of the western United States increasingly vulnerable to wildfire, drought, and insects. Forest managers are trying to improve resilience using treatments such as mechanical thinning and prescribed fire; however, operational and resource constraints limit treatments to a fraction of the needed area each year. An alternative is to let wildfires burn under less-than-extreme fire weather where human lives and infrastructure are not at risk. We examined post-fire forest structure using airborne lidar data to determine whether a single wildland fire following an extended fire-free period could produce forest structures resembling fire-resilient historical conditions. We studied forest structures resulting from these "first-entry" fires in a forest with a history of timber management (2008 American River Complex Fires, Tahoe National Forest) and in a wilderness area (2009 Big Meadow Fire, Yosemite National Park). We compared the results of these first-entry fires with nearby reference areas that had experienced 2+ fires that burned predominately at low- and moderate-severity. We identified visible overstory trees from the lidar data and examined their patterns in terms of individuals, tree clumps, and openings. We found that moderate-severity fire effects in these first-entry fires produced similar patterns to the reference areas with area in openings at approximately 40% and trees predominately in small (2 to 4 trees) and medium (5–9 trees) clumps High-severity fire produced mortality likely to lead to large canopy openings that were historically uncharacteristic in these forests. As burn severity increased, the amount of the residual canopy area represented by taller trees (> 16 m and especially > 32 m) decreased, which could result from fires preferentially killing taller trees or from locations with taller trees more commonly experiencing lower burn severities. Our study suggests that first-entry fires allowed to burn under less-than-extreme conditions can reproduce spatial patterns resembling historical conditions resilient to fires and drought but possibly at the disproportionate expense of larger trees.

1. Introduction

Over a century of fire suppression, timber harvesting, and other management practices have left the previously frequent-fire forests of the western United States increasingly vulnerable to wildfire, drought, and insects (Franklin and Johnson, 2012; Stephens et al., 2016). Wildland fire coupled with climatic change threatens critical habitats, healthy water supplies, residential safety, carbon storage, and recreational amenities (Lalonde et al., 2018; Liang et al., 2018). These threats are likely to grow over time as fuel loads increase, temperatures warm, and drought becomes more frequent (Abatzoglou and Williams, 2016; Crockett et al., 2018; Diffenbaugh et al., 2015; Stephens et al., 2008; Stephens et al., 2018; van Wagtendonk and Moore, 2010).

To address the increased vulnerability of altered forests to a changing climate, managers are focusing on improving resilience. We use ecological resilience (hereafter, resilience) to refer to the capacity to persist through and re-organize after disturbance, adapt to shifting environmental conditions, and maintain basic ecosystem structure and function over time (Walker et al., 2004). Increasingly, the spatial patterns of trees and openings within stands are considered in developing restoration guidelines (Churchill et al., 2017). Historically, repeated low- to moderate-severity fires organized forests into patterns of individual trees and distinct small tree clumps separated by openings of varying sizes (Churchill et al., 2013; Larson and Churchill, 2012; Barth

* Corresponding author at: University of Washington, Box 352100, Seattle, WA 98195-2100, USA.
E-mail address: vkane@uw.edu (V.R. Kane).

https://doi.org/10.1016/j.foreco.2019.117659
Received 3 July 2019; Received in revised form 29 September 2019; Accepted 30 September 2019

et al., 2015; Jeronimo, 2018; Jeronimo et al., 2019; Kane et al., 2014; Larson and Churchill, 2012; Lydersen et al., 2013). Heterogeneous patterns of trees and openings create a patchy surface fuel matrix that burns with more variable fire behavior, reduced crown fire potential, and reduced large tree mortality compared to the dense, closed-canopy forests common following fire suppression (Bigelow et al., 2011; Kennedy and Johnson, 2014; Linn et al., 2013; Miller and Urban, 2000; Parsons et al., 2017; Rothermel, 1991; Safford et al., 2012; Stephens et al., 2008; Symons et al., 2008; Ziegler et al., 2017). The reduced tree density created by interspersed openings also reduces the risk of subsequent drought mortality (Knapp et al., 2017; Skov et al., 2004; Stephens et al., 2008; Stephens et al., 2018; Young et al., 2017). In addition to conferring resilience, greater variability in tree clump sizes improves habitat for a range of wildlife species (Buchanan et al., 2003; Comfort et al., 2016; Daw and DeStefano, 2001; Hollenbeck et al., 2011; Roberts et al., 2008; Sollmann et al., 2016, 2015).

Lydersen et al. (2013) among others documented the loss of this historical structure and the resulting homogenization of spatial pattern under a regime of overstory harvest followed by decades of fire suppression. Managers are beginning to use combinations of mechanical thinning and prescribed fire to restore these historical spatial patterns (Churchill et al., 2017). However, treatments are often constrained due to a lack of resources and conflicting management goals, limiting the area treated to a small fraction of that needed each year to meaningfully reduce fire hazard (North et al., 2012; Stephens et al., 2016; Vaillant and Reinhardt, 2017). As an alternative, wildfires could be managed in a way that would allow restoration of resilient tree clump and opening patterns while also reducing fuels. This strategy, for example, has been successfully adopted in Yosemite and Sequoia-Kings Canyon National Parks where substantial areas have had two or more low- or moderate-burn severity fires (Jeronimo et al., 2019; Kane et al., 2014).

No study that we aware of, however, has examined whether first-entry, or initial, burns following decades of fire suppression recreates opening and tree clump patterns resembling those likely produced by historical frequent burns at low- to moderate-severity. If first-entry burns were shown to produce these structures, which likely would increase resilience to future fires and drought, then managers may be more willing to allow fires burning under low- and moderate-fire weather to burn.

In this study, we used airborne lidar (formerly an acronym for 'light detection and ranging') data to examine forest structures resulting from two fires in the Sierra Nevada, California, USA. Airborne lidar data allows high fidelity measurement of overstory tree structure over large areas (Kane et al., 2010a,b) and has been used to study the effects of fire across landscapes in the Sierra Nevada (García et al., 2017; Hu et al., 2019; Jeronimo et al., 2019; Kane et al., 2013, 2014, 2015a,b). One of our study fires burned in a forest with a history of active timber management and the other in an area with no harvest history. Both fires include control areas where this fire was the first-entry fire with no record of previous fires since 1878. We compare the mixture of forest structures created by different burn severities in these fires to nearby reference areas that have experienced two or more predominately low- to moderate-severity fires, as well as nearby the control areas. In this paper, we address four questions:

- How do patterns of tree clumps and gaps vary by burn severity?
- Does the distribution of overstory tree heights change with increasing burn severity?
- How does a first-entry fire change forest structure in managed versus wilderness forest?
- Do the changes from first-entry fire move structure toward a contemporary active-fire reference condition?

2. Methods

2.1. Study areas

Our study areas were located in the Sierra Nevada mixed-conifer zone, which is dominated by a variable mix of ponderosa pine (*Pinus ponderosa*), Jeffrey pine (*P. jeffreyi*), sugar pine (*P. lambertiana*), white fir (*Abies concolor*), red fir (*A. magnifica*), and incense cedar (*Calocedrus decurrens*). Common hardwood species in these forests include black oak (*Quercus kelloggii*) and canyon live oak (*Q. chrysolepis*). We limited our analysis to the lower montane, mid-montane, and upper montane climate classes associated with this zone mapped by Jeronimo et al. (2019). Historically, these forests had a frequent, predominantly low-severity fire regime, and are a focus for restoration to improve their resilience to fire following nearly a century of fire suppression (Weatherspoon and Skinner, 1996; North et al., 2009).

We selected two fires that 1) had an area for which the fire was the first recorded fire, 2) burned with a mixture of burn severities, 3) and had post-fire airborne lidar coverage (Fig. 1). We determined whether an area had previously burned or not by using the California State Fire and Resource Assessment Program's maps of fire perimeters extending back to 1878 (http://frap.fire.ca.gov/data/frapgisdata-sw-fireperimeters_download; accessed June 7, 2019). In addition, both fires included areas where two or more predominantly low- to moderate-severity fires had occurred that we used as reference areas (Jeronimo 2018; Jeronimo et al. 2019). To evaluate what the pre-fire forest structure might have been in the first-entry burn areas, we selected nearby control areas that had no record of fire.

To determine that the areas of the first-entry burns and the controls had similar pre-fire forest structures, we compared pre-fire values for basal area, quadratic mean diameter, and canopy cover as modeled by the Landscape Ecology, Modeling, Mapping, and Analysis program (Pierce et al., 2009) (https://lemma.forestry.oregonstate.edu/data; accessed June 7, 2019). We determined that the areas were not statistically distinct using the Kolomogorov-Smirnov test (Lilliefors, 1969, 1967) using the R statistical software (R Core Team, 2013), which is a nonparametric test that quantifies the distance between two cumulative distribution functions for continuous values. We removed from the analysis areas within the first-entry burns and the control areas that were not identified as having conifer or mixed-conifer vegetation cover in the USDA Forest Service's Existing Vegetation (eVeg) classification database. (https://www.fs.usda.gov/detail/r5/landmanagement/resourcemanagement/?cid=stelprdb5347192 accessed August 15, 2019). The two study areas differed by size and range of and mean elevation (Table 1).

For the fire in an area with a history of active management, we selected the lightning-ignited 2008 American River Complex (ARC) Fires in the Tahoe National Forest. In the mid to late 1800s, large portions of this area were largely clear cut, in the 1970s and 1980s numerous clear cuts and shelterwood cuts were done across the fire area, and in the years before the fire several fuel treatments were implemented (Safford, 2008). The center portion of the fire's area is managed as a designated roadless area, which means that little to no management activities have occurred in recent decades. Both the first-entry burn and control areas have been subjected to active management in the decades leading to the ARC fires. The USDA Forest Service's Activity Tracking System (FACTS) (https://data.fs.usda.gov/geodata/edw/datasets.php?dsetParent=Activities; accessed August 15, 2019) shows that 18% of the control area and 19.5% of the first-entry burn area had had a variety of management activities from 1968 through the time of the fires.

The ARC Fires burned approximately 8100 ha between June 21 and August 1, 2008. These began as several individual fires that merged into a contiguous area, and we analyze them as a single fire. Management activities to suppress the fire were limited by available resources (over 2000 fires were ignited statewide that summer) and smoke-induced

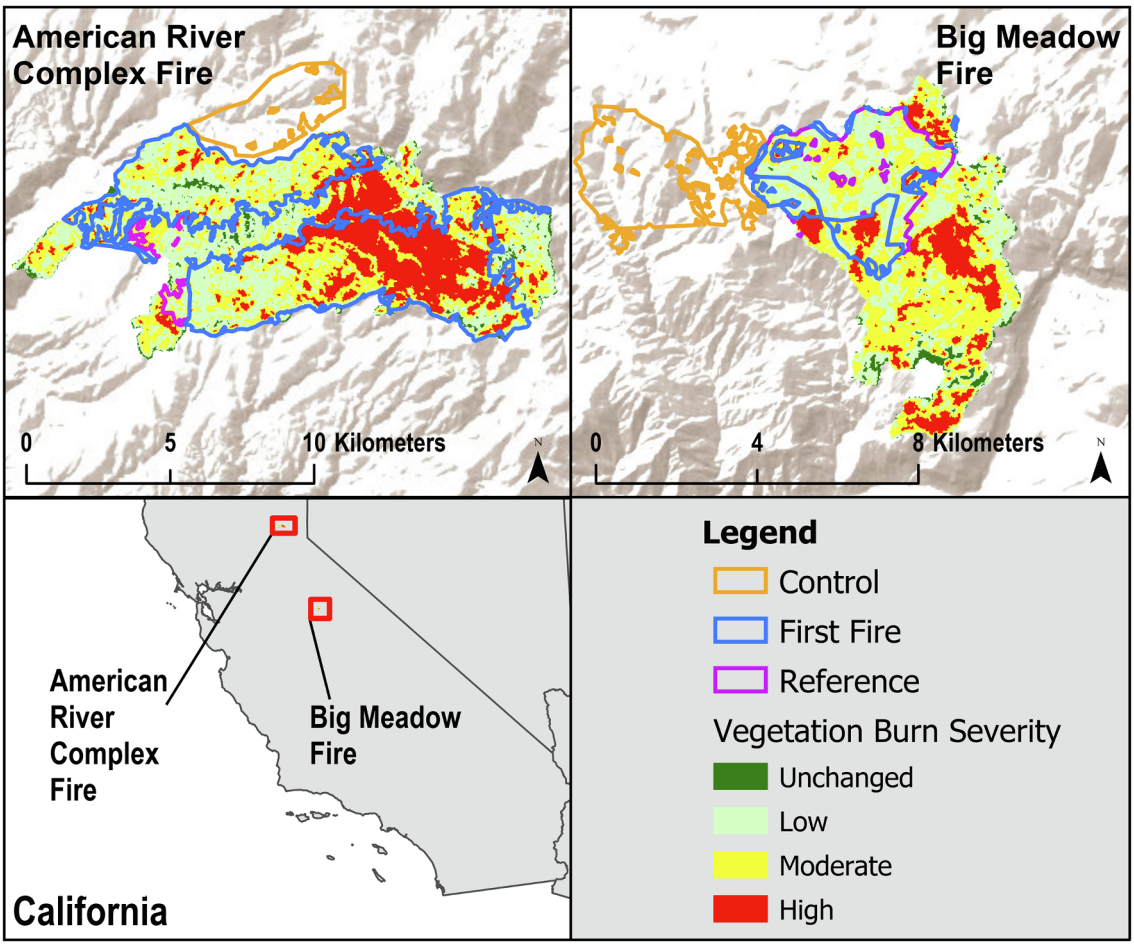

Fig. 1. Study area locations for the 2008 American River Complex Fires in Tahoe National Forest and the 2009 Big Meadow Fire in Yosemite National Park. Each study fire included a first-entry burn following decades of fire suppression, one or more adjacent reference areas that experienced two or more predominately low- and moderate-severity fires, and a nearby control area that has no recorded history of fire.

limitations on air operations (Safford, 2008). These resource limitations and the relatively benign fire behavior contributed to the long duration of the fire. Most of the area with high-severity fire burned over two days under extreme fire weather when values for the Energy Release Component (ERC, a measure of fuel dryness) exceeded 90th percentile values. We excluded from our study area a portion of the ARC Fires that had previously burned (and did not meet reference forest criteria, (Jeronimo et al. 2019) and portions that were not classified as conifer or mixed-conifer vegetation types in the eVeg database

For the fire in an area with no harvest history, we selected the 2009 Big Meadow Fire in Yosemite National Park, which resulted from an escaped prescribed fire (National Park Service, 2009). This fire burned 3004 ha between August 26 and September 10, 2009. The National Park Service has managed this area as wilderness (and a portion of the area is congressionally designated wilderness) with no record of pre- or post-fire logging. Following the escape of the prescribed fire, park managers worked to actively suppress and contain the fire. We excluded from our study area portions of the Big Meadow Fire that had previously burned in the predominately high-severity 1990 A-Rock Fire, burned in the 2013 Rim Fire, or lay outside the area of the lidar coverage.

Because of the complex fire histories of both study areas and the area available within each lidar flight, we were constrained in selecting the location of adjacent control and reference areas. This led to differences in mean elevation between these control areas and the areas of the first-entry fires, particularly for the ARC Fires (Table 1). In addition, the ARC Fires' control area was located around a ridge while that fire primarily burned valley slopes in the conifer and mixed-conifer vegetation zones included in this study.

The choice of the location for the Big Meadow Fire control area was constrained by available lidar data coverage and the fire history of the nearby areas. We chose an area that had experienced some harvesting

Table 1
Area in hectares and elevation ranges for each study area's reference and control areas, and the first-entry low-, moderate-, and high-severity burn areas.

	American River Fires					Big Meadow Fire				
	Ref.	Control	Low	Mod.	High	Ref.	Control	Low	Mod.	High
Area (ha)	135	912	1792	1758	1424	780	926	131	139	89
Elevation (m)										
Minimum	767	1465	718	731	740	1642	1586	1492	1456	1491
Mean	1333	1724	1474	1543	1598	1941	1801	1833	1761	1751
Maximum	1641	2102	2059	2056	2044	2161	2004	2158	2145	2107

up to the 1920s prior to being incorporated into the park. In selecting this area, we examined both the canopy areas of lidar identified trees based on tree heights (see methods below) and the distribution of these values as examined by niche overlap analysis (Broennimann et al., 2012; Mouillot et al., 2005) between the control area and areas that experienced low-severity burns in the Big Meadow Fire. By both measures, the control area had far fewer identified trees > 48 m than the low-severity burn patches but similar canopy area for trees in the 32 m to 48 m stratum. This would be consistent with the control area having been harvested through removal of the largest trees ('high grading'), which was a common practice in that era in the Sierra Nevada. However, since the control area had not been subjected to further active management since the 1920s, we believed that it was representative of the infilling common following decades of fire suppression.

We wanted to compare the effects of the first-entry fires against contemporary reference areas where re-introduced frequent-fire regimes have burned forests following decades of fire exclusion. Unlike reference conditions based on historical field data or reconstructions of historical stands from contemporary field data, modern reference sites reflect post-fire exclusion responses to fire in contemporary climate conditions (Jeronimo et al., 2019). We used the methods of Jeronimo et al. (2019) to identify areas within the ARC Fires and Big Meadow Fire that met the following criteria to be a contemporary reference area: average number of fires is ≥2 although portions with a single fire were permitted, at least one fire within the last 30 years, and high severity burn patches were ≤10% of the area. The Westville and Italian reference areas were identified after the publication of Jeronimo et al. (2019) and lay within the ARC Fires burn perimeter. A large portion of the Big Meadow Fire (780 ha) constituted the Tamarack reference area (Jeronimo, 2018; Jeronimo et al., 2019). Additional information on the characteristics of the reference areas is provided in the online supplement.

2.2. Lidar acquisitions and burn severity maps

The National Center for Airborne Lidar Mapping (Houston, Texas, USA) collected airborne lidar data for both study areas using Optec family lidar sensors that recorded up to four returns per pulse. The Center acquired lidar data covering the ARC study area in 2013, five years after the fires, with an average density of 8.6 pulses per square meter, a scan angle of ± 14°, and a nominal flight altitude of 600 m. The Center acquired lidar data covering the Big Meadow study area in 2013, four years after the fire, with an average density of 12 pulses per square meter, a scan angle of ± 14°, and a nominal flight altitude of 600 m. The time between the fires and the lidar acquisition for both study areas was long enough for needle drop and extended delayed tree mortality following the fire to occur (Hood et al., 2010). We used the vendor-supplied digital terrain models derived from the lidar data.

We used one-year post fire 30 m resolution burn severity maps available from the Monitoring Trends in Burn Severity (MTBS) project (Eidenshink et al., 2007) to estimate burn severity for the ARC and Big Meadow Fires. We used a focal function to average burn severity for a 3 × 3 grid cell area surrounding each focal pattern to match the area of 90 × 90 m analysis windows used to analyze forest structure patterns (see below). We used the Relativized differenced Normalized Burn Ratio, RdNBR, (Miller and Thode, 2007) which is an extension of the differenced Normalized Burn Ratio, dNBR (Key and Benson, 2006). These severity measurements calculate Normalized Burn Ratios (NBRs) from Landsat bands 4 (near infrared) and 7 (mid infrared) using pre- and post-fire images to estimate burn severity. Higher values of these satellite-derived burn indices indicate a decrease in photosynthetic materials and surface materials holding water and an increase in ash, carbon, and soil cover. Miller and Thode (2007) and Miller et al. (2009) demonstrated that RdNBR produced more accurate classifications of fire severity in Sierra Nevada forests, particularly for areas with lower pre-fire canopy cover. We classified the continuous RdNBR measurements into the five standard MTBS fire severity classes using the field validated RdNBR thresholds from Miller and Thode (2007): < −150, enhanced greenness indicating bloom of plant growth; −150 to 68, no detected change in post-fire vegetation; 69 to 315, low-severity burn with fine fuels removed and some scorching of understory trees; 316 to 640, moderate burn severity with some fuels remaining on forest floor, mortality of small trees, scorching of crowns for medium and large-sized trees; and ≥641, high burn severity with near-complete combustion of ground fuels, near total mortality of small and medium sized trees, and severe needle scorch and/or mortality of large trees.

2.3. Lidar processing

We created canopy height models (CHMs) for the study areas using the US Forest Service's FUSION Lidar Toolkit (McGaughey, 2018). Lidar return heights were normalized using the vendor-delivered ground models. The CHMs were created as a 0.75 m resolution raster in which each cell took on the z-value of the highest lidar return in that cell above the elevation of the digital terrain model. The CHM was smoothed with a 3x3 cell mean filter to remove noise and to improve overstory tree detection (Jeronimo et al., 2018; Jeronimo, 2015).

Individual trees in the overstory were identified using the FUSION TreeSeg tool, an implementation of the watershed transform algorithm (McGaughey, 2018; Vincent and Soille, 1991). We identified trees using only CHM grid cells > 2 m in height to exclude the ground and shorter shrubs and trees. Each identified tree was assigned a georeferenced x,y-location and a height corresponding to the highest CHM grid cell in its identified crown. The TreeSeg algorithm examined the morphology of the canopy surface model surrounding the high point of each identified tree to model the crown perimeter of the tree, which was stored as a polygon (McGaughey 2018). We chose the watershed algorithm because it is a mature algorithm, is computationally efficient over large areas, and is implemented in several lidar processing packages making it easy for others to follow our methods. Its accuracy also has been assessed in Sierra Nevada mixed-conifer forests (Jeronimo et al., 2018; Jeronimo, 2015).

The watershed transform algorithm, like almost all lidar tree identification algorithms, identifies overstory trees directly visible to the lidar instrument. Subordinate trees, which often are the most numerous on a site, are not detected. We adopt the tree-approximate object (TAO) paradigm where each TAO represents an identified tree that may have none to several subordinate trees beneath its outer surface (Jeronimo et al., 2018; Jeronimo et al., 2019; North et al., 2017). Treating tree detection results as TAOs is a way to make use of tree-scale measurements while explicitly recognizing that subordinate trees are not identified.

2.4. Analysis of openings, tree clumping, and tree height patterns

We identified individual TAOs and clumps of TAOs using the Individuals, Clumps, and Openings (ICO) tree spatial analysis pattern method (Churchill et al., 2013) adapted for use with airborne lidar data (Jeronimo et al., 2019; Wiggins et al., 2019). Our algorithms identified TAOs as members of the same tree clump if a circle centered on the TAO high point with the same area as the modeled tree crown area touched or overlapped (Fig. 2). This approach allowed for the distance between TAO high points to vary based on the morphology of the crown surrounding the high points.

We used canopy area as a surrogate for ecological influence of TAOs and clumps. In this way, we integrated both the canopy size of trees within clumps (with taller trees tending to have larger canopy areas) and the number of trees within clumps in our analysis. Clump size distributions were reported as the summed canopy areas of TAOs in clumps of different sizes: individuals, small clumps (2 to 4 TAOs), medium clumps (5 to 9 TAOs), large clumps (10 to 29 TAOs), and mega

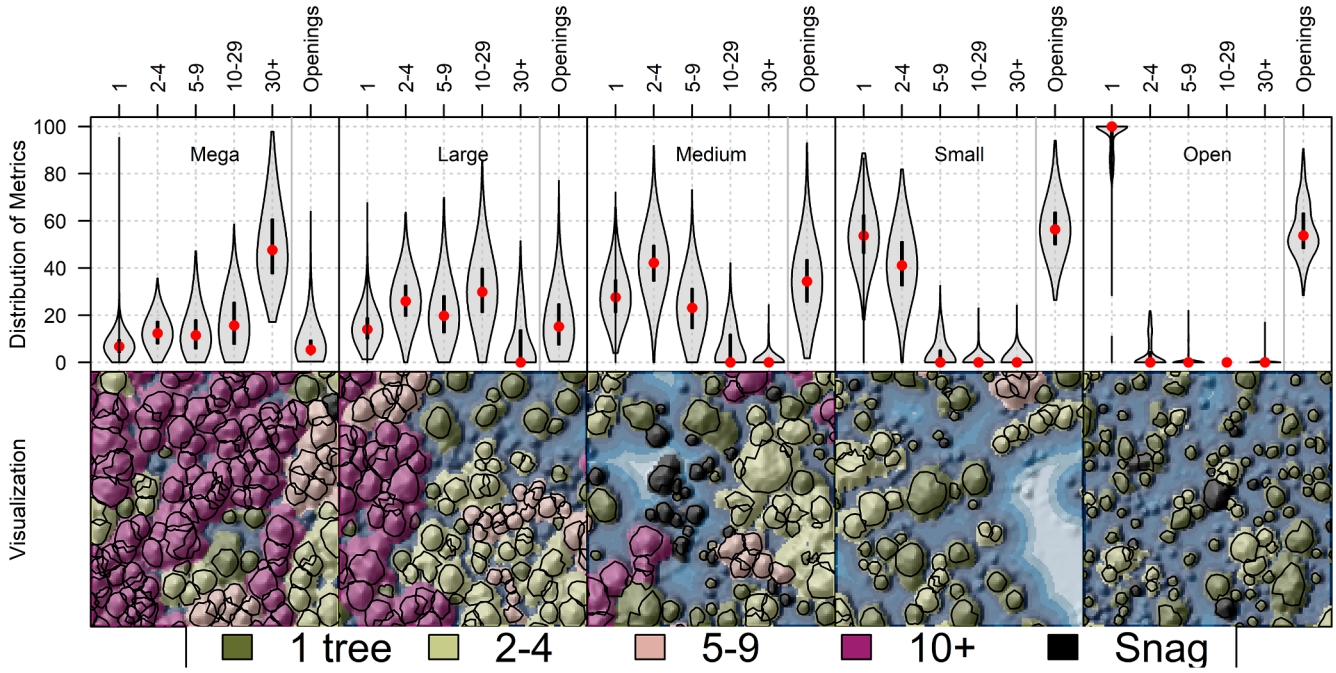

Fig. 2. Visualization of tree approximate object (TAO) clump and opening patterns for 90 m × 90 m areas identified in this study and of the TAO clumping structure classes identified. The distribution of values for the proportion of canopy area in each clump class is shown in violin plots. Names for each class reflect the dominant tree clump sizes: open area dominated by individual TAOs, small clumps (2 to 4 TAOs), medium clumps (2 to 4 and 5 to 9 TAOs), large clumps (10 to 29 TAOs), and mega clumps (≥30 TAOs). Classes were defined by the percentage of canopy cover > 2 m in each clump size and percentage of open space in each 90 × 90 m grid cell. Clump size ranges for each violin plot shown above figure. Black lines show the modeled TAO canopy boundaries. Violin plots show the distribution of values for grid cells in each tree clump size class, with dots depicting the mean value, lines showing the extent of the 25th to 75th percentile range, and width showing the frequency of values.

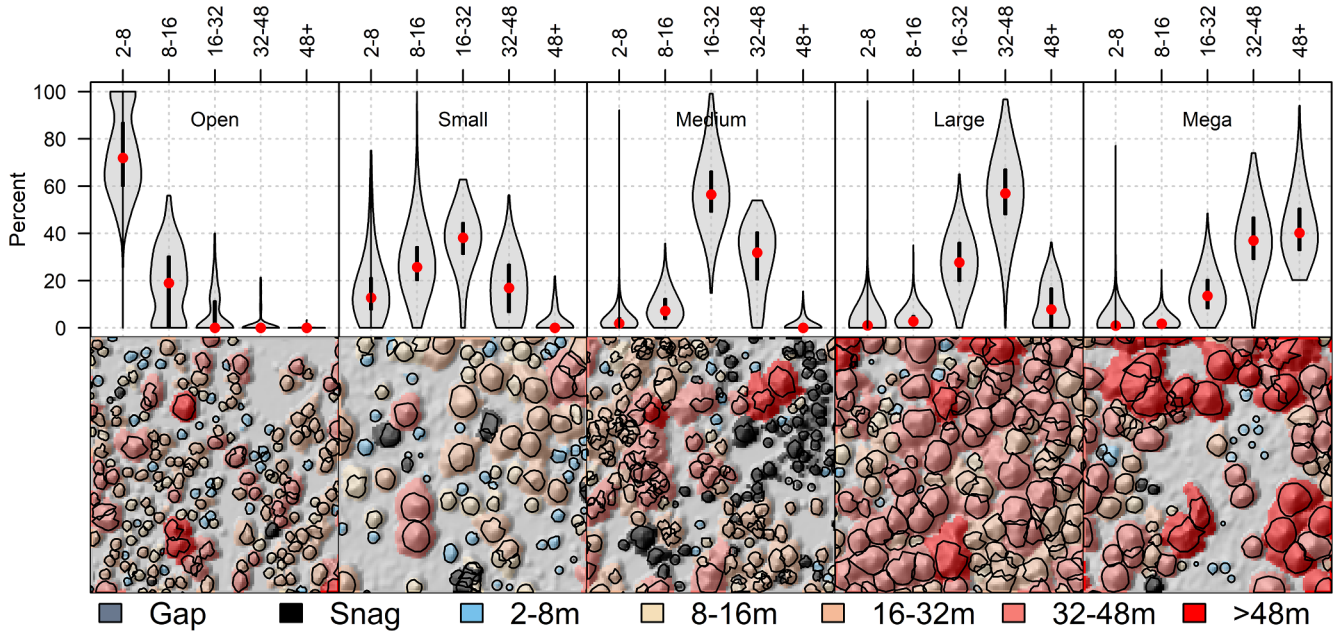

Fig. 3. Visualization of tree approximate object (TAOs) heights for 90 m × 90 m areas identified in this study and of the TAO height structure classes identified. The distribution of values for the proportion of canopy area in each clump class is shown in violin plots. Names for each class reflect the dominant height by strata sizes. Classes were defined by the percentage of canopy cover > 2 m within each height strata. Stratum height ranges for each violin plot shown above figure. Violin plots show the distribution of values within each height strata, with dots depicting the mean value, lines showing the extent of the 25th to 75th percentile range, and width showing the frequency of values.

clumps (≥30 TAOs).

We similarly aggregated TAO heights by bins and reported the canopy area for each height stratum: shortest (dominated by TAOs 2 m to 8 m), short (8 m to 16 m), mid height (16 m to 32 m), tall (32 m to 48 m), and tallest (> 48 m) (Fig. 3). The entire modeled canopy area for each TAO was assigned the height of the highest point within the TAO. With increasing burn severity, the total canopy area would generally be expected to decrease leading to reduced canopy area for each stratum. To normalize for this expected difference in total canopy area, we report canopy area by stratum as a percentage of total canopy.

We identified TAOs that were likely to be snags using lidar intensity values. We identified likely snags as TAOs whose first lidar return mean intensity value fell in the lower 25% range of mean intensity for all TAOs. The mean intensity range was scaled to the 1st to 90th percentile range to exclude abnormally high values. We adopted this heuristic because there were no concurrent field or aerial orthographic imagery available to use as training data for snag modeling. Our analysis of other areas with concurrent imagery (data not shown) and the work of others (Casas et al., 2016; Wing et al., 2015, Brian Wing personal communication August 14, 2017) suggests that TAOs with these lower mean intensities are likely to be snags and therefore not part of the living overstory. Similarly, work using the normalized difference vegetation index (NDVI) from hyperspectral data (which uses the near-infrared band along with the red band) found that the 20th percentile break distinguished living and dead canopies (Brodrick and Asner, 2017; Paz-Kagan et al., 2018). We likely only detected TAOs that recently became snags. Snags old enough to have lost most or all their branches were unlikely to have been identified with the watershed transformation algorithm we used; these likely would have been identified as open areas

2.5. Trends in TAO height, tree clump size, and opening area by burn severity

We calculated tree clump, TAO height, and opening patterns across the entirety of each study area. Several studies have found that characteristic tree clump and opening patterns emerge at scales of 0.5 to 4 ha (Churchill et al., 2017; Harrod et al., 1999; Larson and Churchill, 2012; Lydersen et al., 2013). We therefore analyzed these patterns at a 90 m^2 (0.81 ha) scale. We measured the area in each height stratum using a moving 90 × 90 m window with measurements centered at 30 m spacing to match resolution of the burn severity maps. The use of an overlapping moving window had the practical effect of smoothing the measurements of tree clump and opening areas and matched the smoothing performed on the burn severity data.

We reported as open space any area with no vegetation taller than 2 m according to the CHM. Open areas > 9 m from any vegetation > 2 m in height was identified as a core opening. This represents the amount of stand area in openings large enough to subside most crown fires, regenerate shade-intolerant species, and dissipate beetle aggregation pheromones (Churchill et al., 2017). Preliminary analysis showed that the presence of likely snags strongly reduced the area in openings and core openings. As these likely snags decay and fall, the area in openings is likely to increase. We therefore separately report the area in current openings (that is areas with no canopy > 2 m or likely snags) and as possible future openings by including the area of likely snags as openings.

For tree clumps, TAOs, and openings on the edge of a 90 × 90 m analysis area, our algorithm identified whether a clump or opening extended beyond the focal grid cell. It added to the focal grid cell the proportion of that clump or opening within the focal cell for the size of the entire clump or opening. For example, if a clump of eight TAOs was one-third within a grid cell, we added that one-third of the clump area to the total area of medium-sized clumps (5 to 9 TAOs) for that grid cell.

We analyzed the distribution of TAO heights, clumps, and openings within 90 × 90 m analysis windows by burn severity class. We also report the mean values for these metrics in the reference and control areas. We compared mean area and distribution of values for openings, core openings, and snags, along with the canopy area in each tree clump size class and TAO height class between the reference area, the control and each classified level of burn severity. Because of our large sample sizes, all differences in means would be statistically significant. We instead tested for statistical significance of the cumulative distribution of values for pairwise comparisons using the Kolmogorov-Smirnov test (Lilliefors, 1967).

We found that all pairwise distributions were statistically significant at the equivalent of $p < 0.05$ using the Kolomogorov-Smirnov test (Lilliefors, 1969, 1967). We therefore also used niche overlap analysis (Broennimann et al., 2012; Mouillot et al., 2005) to examine whether the distributions were meaningfully different, in addition to significantly different, between pairwise distributions for a metric (for example, percent area in openings; Appendix Fig. A1). Smaller overlaps indicated that distributions were more distinct between pairwise contributions. We are not aware of a published critical value for a difference in niche overlap values being meaningfully different. Based on our use of this analysis from past (for example, North et al., 2017) and current studies, we selected < 80% niche overlap as signifying meaningfully different distribution of values between pairwise comparisons.

2.6. Structure classes of dominant TAO height and clump size

Forests are often complex assemblages of trees in different heights, different sized tree clumps, and different amounts of area in openings at multiple scales. We therefore defined structure classes for both tree clump size distributions and TAO height distributions to capture these combinations of features. We used hierarchical clustering with the Ward.D2 method and the hclust function of the R statistical package (R Core Team, 2013). Trends in dominant TAO heights were summarized using the percentage of canopy area in each height strata within our 90 × 90 m analysis windows, while the clumping structure classes were defined using the percentage of area in different sized tree clumps and total area in openings with our 90 × 90 m grid cells. We used the same tree clump size classes and height strata bins used for our analysis of tree spatial pattern and height analysis (Section 2.4). We used 30,000 random samples from across the control, reference, and burn areas for the hierarchical clustering, and selected the most parsimonious grouping of structure classes that retained most of the original information (McCune and Grace, 2002).

3. Results

3.1. Trends in tree clump size, openings, and tree height with burn severity

The trends for each fire considered separately for openings and canopy area in different clump sizes were similar with increasing burn severity (Fig. 4). The absolute means also tended to be similar. For example, mean area for each fire for openings and snags (possible future openings) increased approximately linearly for both fires with increasing categorical burn severity. In some cases, such as current core openings and possible future openings, the mean values for each burn severity were nearly identical across fires. In other cases, such as the mean opening area with burn severity for each fire, the overall trend was similar, but the values diverged with the Big Meadow fire having lower mean values for moderate- and high-severity burn patches than the ARC Fires.

For both fires, the area in openings increased approximately linearly with increasing burn severity. However, the mean area increases in core openings was only a few percent above zero. It is likely that core opening area would increase in future (up to approximately 40% of the area of high-severity patches) as fire-killed trees fall. The canopy area for individual trees increased with increased burn severity while the canopy area for tree clumps larger than five TAOs decreased with increasing burn severity. The canopy area in tree clumps of 2 to 4 TAOs increased for moderate-severity burns relative to low-severity burns but decreased for high-severity burns.

Generally, the mean values for openings and canopy area in different TAO clump sizes for each fire fell between the mean values for each fire's low- and moderate-severity burn areas although they tended to be closer to the mean values for moderate-severity burn areas. When comparing the first-entry burn areas to their control areas, two patterns emerged. The control area for the Big Meadow Fire had a smaller area

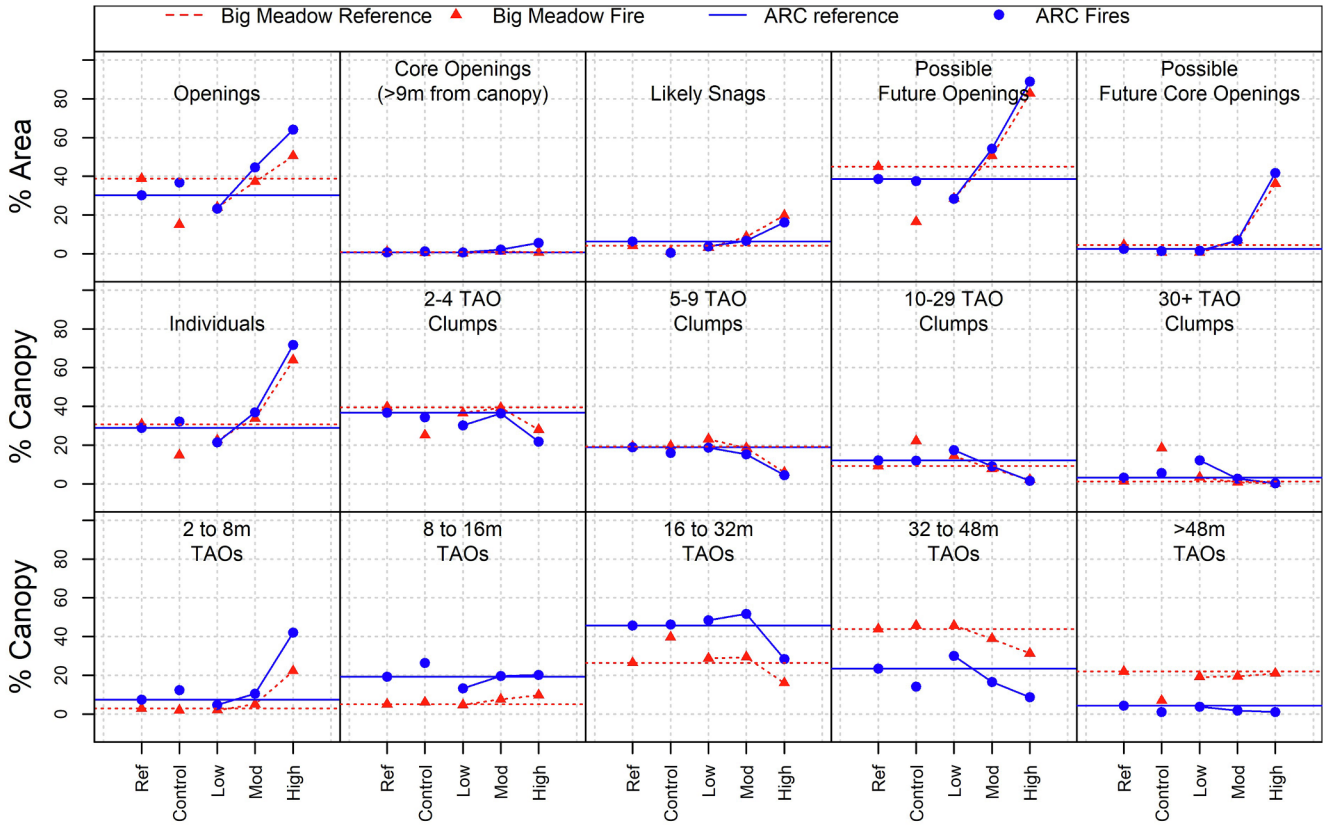

Fig. 4. Mean area in openings, canopy area in different tree clump sizes (based on number of tree approximate objects (TAOs) per clump), and canopy area in different height strata of TAOs (lidar-identified overstory trees) among different classified burn severities and control areas relative to reference areas (horizontal lines) for each study site. Open and core open areas shown both for current conditions and as potential future area by counting area currently classified as likely snags as potential future open areas. Mean values are shown; pairwise distributions of all values are distinct at the equivalent of $p < 0.05$ using the Kolmogorov-Smirnov test. Percent area of openings and snags are relative to the total area of each 90 × 90 m grid cell, while percent area for tree clump and TAOs by height strata are relative to the total area in canopy > 2 m within each analysis window. Core openings refer to area > 9 m from a canopy edge. Appendix Fig. A1 shows a more detailed version of this data.

in openings, less canopy area in individual TAOs and in clumps of 2 to 4 TAOs, but more canopy area in clumps of 5 and greater TAOs than for any of the first-entry burn severities. In general, the Big Meadow Fire's control area had less area in openings, less canopy area in clumps of 4 or fewer TAOs, and more area in clumps of 5 or greater TAOs than its reference area. However, the ARC Fires' control area had greater area in openings, more canopy area in individual TAOs and clumps of 2 to 4 TAOs, and less canopy area in clumps of 5 and more TAOs than the first-entry, low-severity burn areas. In general, the ARC Fires' control area had values similar to the ARC Fires' reference areas.

While the patterns in mean area within openings and tree clumps generally showed clear trends, pairwise niche overlap analysis often showed > 80% overlap in the distribution of values for area in openings and core openings and canopy area in different clump sizes between the control areas, reference areas, low-severity patches, and moderate-severity patches (Appendix A, Fig. A1). This reflects the wide distribution of values for area in openings and different clump sizes for the reference areas, control areas, and different first-entry burn severities. The changes with increasing burn severity, therefore, are best thought of as shifts in the distributions of values rather than as distinct ranges of values associated with each burn severity.

The two study areas differed in the distribution of TAO heights and resulting proportion of the canopy area. The Big Meadow study area had a larger proportion of canopy area in TAOs > 32 m in height than did the ARC study area, and the ARC study area had a larger proportion of canopy area in TAOs < 32 m. Mean proportional canopy area for TAOs in all strata > 16 m generally declined for both fires relative to the control areas and with increasing burn severity. Canopy area for TAOs 2–8 m showed an increase in proportional canopy area with burn severity, especially for high burn severity. However, as with openings niche overlap analysis often showed > 80% overlap for the distribution of the percentage of canopy area in each height stratum between the control area, reference area, and different burn severities.

3.2. Clump and height structure classes

We identified five structure classes by dominant clump size and opening area, and by dominant TAO height strata (Figs. 2 and 3). Examining patterns of clump size structure classes by burn severity showed the same general patterns as examination of the mean values described above with increasing burn severity resulting in a greater proportion of classes of smaller tree clump sizes (Fig. 5). However, the classes revealed patterns of structural heterogeneity not apparent from trends in mean values. While each class had a dominant clump size or height strata, each also included a range of other clump sizes and TAO heights showing structural complexity within the scale of our 90 × 90 m analysis windows. In addition, low- and moderate-severity burn patches were characterized by a mix of several clump size structure classes indicating greater structural complexity than high-severity burn patches, which were dominated by the open clump classes. The ARC Fires' control area had a greater proportion of area in the small and medium but a smaller proportion in the large and mega clump structure classes than did the area of first-entry low-severity burns. The Big Meadow Fire's control area, however, had a smaller proportion of area in the medium but greater proportion in the large and mega clump structure class than the area of the first-entry low-severity burns.

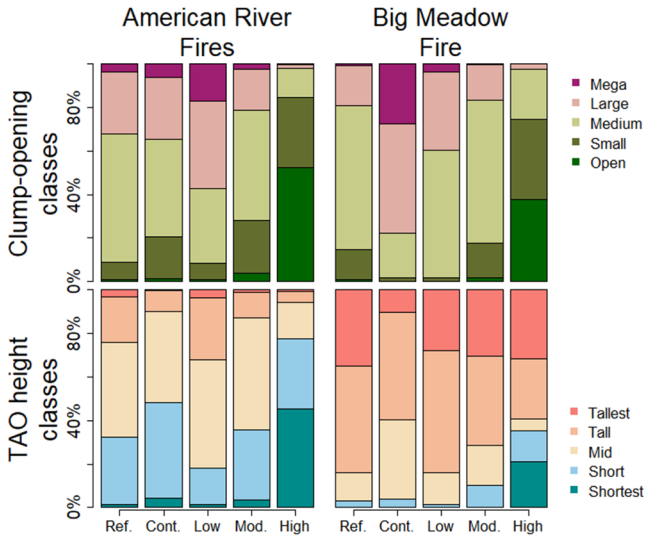

Fig. 5. Percentage of area for structure classes defined as the area in openings and proportion of canopy area in different clump sizes and proportion of canopy area in tree approximate objects (lidar-identified overstory trees) in different height strata). Characteristics of the classes are shown in Figs. 2 and 3.

For the Big Meadow study area, most of the area was in the mid-height, tall, and tallest structure classes in the control area, reference area, and for all burn severities except high severity (Fig. 5). For the ARC Fires, most of the area was in the short, mid-height, and tall classes for the control area, reference area, and for all burn severities except high severity. For both fires, the area in the shortest class was highest in high severity burn patches.

4. Discussion

We found that a single fire burning at moderate-severity can create stand structures in fire-suppressed forests that resemble the fire resilient structures historically created by frequent low- and moderate-severity fires (Lydersen et al., 2013) or by two or more low- and moderate-severity contemporary fires (Jeronimo et al., 2019). Moderate-severity fire appears to create interspersed patterns of openings and tree clumps by acting in a patchy fashion, removing overstory trees and/or leaving snags in discrete patches, while leaving a matrix of relatively intact overstory. For example, we found a substantial increase in open area with first-entry burn severity without a substantial increase in core opening area (Fig. 4, Appendix Fig. 1). This is consistent with fire creating or expanding small openings similar in scale to small tree clumps, as opposed to removing all trees in larger patches resulting in large increases in core openings. The resulting small openings often appear sinuous as opposed to round in visualizations (Figs. 2 and 3). Further evidence for fire causing mortality in a patchy pattern comes from the general stability of TAO height distributions between the reference areas and low- and moderate-burn severity patches. This is consistent with fire leaving or removing entire clumps of overstory trees; fire alternatively could have thinned overstory trees from below.

Moderate-severity burns best produced this fine-scale texture of openings and small- to medium-sized clumps for both our study fires and the reference area. Kane et al. (2014) also saw this pattern across a number of fires they studied using airborne lidar data in Yosemite National Park. These similar results suggest this is an underlying principle of fire behavior that becomes apparent when spatial patterns within first-entry burns of small tree clumps and openings are examined over a sufficiently large enough area. The results of this study suggest this effect may be relatively independent of management history or dominant tree size, at least for historically frequent-fire forests following reintroduction of fire after decades of fire suppression.

While changes in structure generally followed expected directions of change with increasing burn severity (for example, the area in openings increasing with burn severity), the large overlap in structure between the low- and moderate-severity burns, which were both similar to the reference areas, surprised us. We found this in both the overlapping frequency of structure classes for these areas (Fig. 5) and in the frequency in which pairwise comparisons showed > 80% niche overlap in the distribution of values for individual metrics (Appendix, Fig. 1). Put another way, low- and moderate-severity burns don't produce distinct forest structures but differ in the resulting proportion of those structures (Fig. 5). This implies that even low-severity burns, as well moderate-severity burns, can produce similar forest structure to what is present in reference areas that have experienced ≥2 fires. In contrast, high-severity burn patches were distinct with their predominance of the open clump structure class.

4.1. Relationship of opening and clumping patterns with burn severity

In forests with intact historical or restored frequent fire regimes, patterns of individual trees and small tree clumps within a matrix of open space are common across a wide range of regions including those of the American southwest (Sánchez Meador et al., 2011; Tuten et al., 2015), the Sierra Nevada (Lydersen et al., 2013), the inland Pacific Northwest (Churchill et al., 2013), and the Rocky Mountains (Clyatt et al., 2016). Churchill et al. (2013) extended the concepts of Plotkin et al. (2002) to quantify forest spatial patterns based on distributions of trees among Individuals, tree Clumps, and Openings, or 'ICO', methodology (Churchill et al., 2017). We used the methods of Wiggins et al. (2019) and Jeronimo et al. (2019) to extend the ICO method to measure overstory tree ICO patterns using airborne lidar. This overcomes a limitation of previous work where the costs of spatially-explicit tree mapping in the field limited the extent of the area studied. For example, the 22 studies included in Larson and Churchill (2012) ranged in total area from 0.2 ha to 7.3 ha. We used the large area, high-fidelity measurements afforded by airborne lidar to provide lidar-based ICO measurements covering substantial areas of two entire fires, adjacent control areas that lay outside the fire perimeters, and active-fire reference areas. Because our clumps include only overstory trees directly visible to the lidar instrument, the number of trees in our clumps generally will be lower than those from field-based ICO studies that include overtopped trees in clump counts. However, our lidar-based ICO methods provide a way to consistently study large areas for clump and opening patterns and to compare patterns within and between lidar acquisitions.

Numerous studies have observed that unburned forests in the Sierra Nevada are overly dense with nearly continuous canopies following decades of fire exclusion (for example, Fry et al., 2014; Knapp et al., 2017; Lydersen et al., 2013). Each increase in categorical burn severity resulted in an approximately linear increase in mean open area with little to no increase in core gap area for low- and moderate-severity burns. At the same time, the proportion of area in larger clumps showed a modest decline. Together these results suggest that for areas that burned at low- to moderate-severity, patchy removal of trees increased the area in small gaps resulting in the breakup of larger tree clumps while creating little new core gap area.

Low- and moderate-severity burns generally produced opening and clumping patterns similar to or bracketing those of the reference areas (Fig. 4) with moderate-severity fires generally producing results closer to the reference areas. Using different datasets (one with lidar and another with forest inventory data) Kane et al. (2014) and Collins et al. (2017a) both concluded that moderate severity fires best approximated forest structure similar to conditions prior to fire suppression. The similarity of reference areas that generally experienced two or more burns and first-entry low- and moderate-severity burns suggests that second low- or moderate-severity fires do little to change the opening and clump patterns created by the first fire. This supports the observation that historical opening and clump patterns created under

frequent-fire regimes create forest structures resilient to subsequent fires (Bigelow et al., 2011; Kennedy and Johnson, 2014; Linn et al., 2013; Miller and Urban, 2000; Parsons et al., 2017; Rothermel, 1991; Safford et al., 2012; Stephens et al., 2008; Symons et al., 2008; Ziegler et al., 2017).

The diversity of clump structure classes associated with the low- and moderate-severity burn patches (and the references areas, which also predominately burned at low and moderate severity) reveals the diversity of stand structures that can result from lower severity fires (Fig. 5). Commonly, Landsat-based burn severities in many studies assume low-severity results in a < 25% canopy cover loss, moderate severity with a 25% to 75% loss, and high severity with a > 75% cover loss, which is consistent with the increase in openings as burn severity increased (Fig. 4). However, the low-and moderate-burn severity classes do not have a single characteristic open and tree clump pattern but are instead characterized by a diversity of structures (Fig. 5). This emphasizes the need to consider disturbance-caused changes to forest spatial structure in addition to broad measures such as canopy cover when assessing the effects of fire.

Only high-severity burns predominately were associated with a single clump structure class, the open structure class with large core openings and TAOs mostly occurring as individuals and in small clumps of 2 to 4 trees. These core areas create the open light conditions commonly needed for pine reproduction (Bigelow et al., 2011; Fowells and Stark, 1965). However, the high light environment also creates conditions in which dense shrub fields can establish that can crowd out tree regeneration (Bohlman et al., 2016; Collins and Roller, 2013; McDonald and Fiddler, 1989; North et al., 2019; Welch et al., 2016) and burn at high severity in subsequent fires killing any trees that did establish between fires (Coppoletta et al., 2016). When openings become especially large, tree regeneration can fail because of the lack of sufficiently close seed sources (Collins et al., 2017b; Shive et al., 2018; Welch et al., 2016). The 25th to 75th percentile values for the area in core openings for high-severity classes ranged from < 50% to > 80% for both fires (Appendix Fig. 1). This indicates that areas estimated to have experienced high-severity burns from Landsat data can have a wide range of structural characteristics and corresponding ecological effects following the fire. Although areas burned at high severity tended to have large open area (Fig. 4), the range in the amount of core open area found in this study supports the notion that the distance to nearest live tree and other factors influencing regeneration potential should be considered in post-fire management within high severity patches (North et al. 2019).

A series of recent studies in Yosemite National Park related to the 2013 Rim Fire suggest potential mechanisms that could have driven the observed changes in clump and opening patterns. Cansler et al. (2019) found that pre-fire, fuel loading spatially varied by an order of magnitude within a 25.6 ha study area, which likely would have led to localized variations in fire intensity and subsequent patterns of tree mortality. Jeronimo et al. (personal communication) analyzed tree mortality using lidar data for the 2013 Rim Fire and found that variation in burn weather and fuel amounts across the fire provided the basic template for mortality levels, while fine-scale (< =0.1 ha) horizontal and vertical canopy continuity accounted for the heterogeneous local distribution of mortality. An examination of the causes of post-fire mortality found that mortality of overstory trees was most strongly associated with interactions between spatially aggregated fire damage, pre-fire competition, bark beetles, and pathogens (Tucker Furniss, personal communication). These three studies suggest that mortality is density-dependent and spatially aggregated, leading to group-scale mortality and survivorship. That is, density-dependent mortality risk is shared among all tree at the scale of small clumps. This is consistent with our finding that, within a burn severity category (which was likely driven by larger-scale factors), individual and clumped tree mortality tended to emphasize pre-fire fine-scale patterns for fuels and tree density and post-fire spatially aggregated mortality agents. These factors would lead to thinning of stands based on small clumps of overstory trees but leaving the TAO height distribution relatively intact for low- and moderate-severity burns.

4.2. Relationship of TAO height with burn severity

We examined the distribution of TAO heights as burn severity increased to determine whether fire was preferentially removing trees in specific height strata, especially larger trees that are disproportionally declining both locally and globally (Lindenmayer et al., 2012; Lutz et al., 2009; McIntyre et al., 2014). With increasing burn severity, the mean proportion of canopy from TAOs > 16 m generally declined (Fig. 4), although niche overlap analysis showed considerable overlap in the ranges of canopy cover by TAO height strata (Appendix Fig. 1). This trend is partially explained by the increase in the mean proportion of TAOs in the 2 m to 8 m stratum, which we believe may have been dominated by regeneration following the fires. However, the importance of tall trees as forest structural keystones (Lutz et al., 2012) makes it important to consider possible ecological causes of the apparent loss of trees in the higher height strata.

The influence of tree size on burn severity provides one possible explanation for the lower proportion canopy area for larger TAOs with increasing burn severity. Other studies have noted that fire severity tends to increase with increased densities of smaller trees (Agee and Skinner, 2005). The increase in high-severity burns in California (Miller et al., 2012; Stevens et al., 2017) likely is in part due to the increase in smaller trees following fire suppression (Collins et al., 2017a; Lydersen et al., 2013) that lead to larger high-severity burn patches (Mallek et al., 2013). This observation means that conversely, a higher proportion of taller TAOs are found in patches of lower burn severity because their presence makes higher severity burns less likely as they are more resistant to fire. A logical consequence of this is that the higher burn severity patches may simply have had fewer large TAOs than lower burn severity patches prior to the fires.

Work by Lydersen et al. (2016), however, suggests that higher burn severities result in the loss of larger trees. They used pre- and post-fire field data for the 2013 Rim fire to examine survivorship rates for different tree sizes. Their results showed that larger diameter trees disproportionally died with increasing burn severity. For example, they found that for low-severity burns, the survival rate for trees 31 cm to 61 cm diameter at breast height (dbh) was 92%, for 61 cm to 91 cm was 97%, and > 91 cm was 79%. Based on allometric equations of dbh to tree height, the corresponding height ranges for these diameter bins would be 15 m to 30 m, 30 m to 43 m, and > 43 m. For moderate severity burns, the corresponding percentages for survivorship were 63%, 68%, and 49% and for high-severity burns 4%, 15%, and 0%.

Our study cannot determine whether the lower canopy area in taller TAOs in high-severity areas is due to a lower incidence of high-severity fire in areas dominated by taller trees or due to mortality of large trees given the available data. In addition, a statistical explanation is that as the canopy area in TAOs 2 m to 8 m increases, this will cause a percentage decrease in canopy area for all other height strata even if the absolute number of larger trees remains the same. As wildfires continue to burn, they are likely to burn networks of previous plots and areas of lidar coverage. We encourage researchers to use these fires as natural experiments and use re-measurements to study this issue in future studies.

4.3. Comparison of clumping patterns

We expected to find differences in the clumping patterns between the Big Meadow and ARC fires based on the different management histories of the two areas. As part of Yosemite National Park, the area of the Big Meadow Fire has been managed as wilderness with no recorded timber harvests. As a result, the area would be expected to have a higher proportion of large trees (Collins et al. 2017a), which was supported by our finding of a much higher proportion of canopy area for

TAOs > 32 m for the Big Meadow study area than for the ARC study area (Figs. 4 and 5). As a result, the spatial patterns of trees in forests with these "legacy" trees in Yosemite would likely retain the imprint of the clump-opening patterns created by the historical frequent fire regime. The area of the ARC Fires, on the other hand, experienced harvests, sometimes multiple, followed by natural regeneration and planting. Both areas experienced over a century of fire suppression, which resulted in densification of the forest, often by species such as white fir that are less fire resistant (Fry et al., 2014; Knapp et al., 2017; Lydersen et al., 2013). We expected the tree clumping patterns to diverge with increased burn severity between the two fires given the greater dominance of shorter TAOs for the ARC Fires than for the Big Meadow Fire. For a given fire intensity, smaller trees with their thinner barks and lower canopies should die with a higher frequency than larger trees. Instead, we found that the opening and clump patterns for burn severities and references for each fire closely mimicked each other both in absolute mean values and in trends of change with increasing burn severity (Fig. 4).

Other studies of frequent fire forests using the ICO method (or similar methods) generally find structures like our reference area and the low- to moderate-severity fire patches. Lydersen et al. (2013) used spatially-explicit stem maps for three plots in the Sierra Nevada from 1929, early in the fire suppression era and before harvest, and in 2007/2008, 78 and 79 years after logging. The 1929 stand structures in Lydersen et al. (2013) resemble those of our restored fire reference stands in terms of area in openings and core openings, and in the distribution of trees across a range of clump sizes, while the 2007/2008 patterns resemble the Big Meadow Fire control area but not the ARC Fires' control area (see Section 4.4). Churchill et al. (2017) reconstructed historical ICO patterns for 14 field plots in the historically fire-frequent Blue Mountains in eastern Oregon, USA. They found much greater area in core gaps than Lydersen et al. (2013) with values ranging from 15% to 72% and with trees predominately as individuals or in clumps of < 9 trees (although the dominant tree clump size varied considerably across plots). Tuten et al. (2015) examined both current and historical spatial patterns for a ponderosa pine forest in northern Arizona, USA. They did not report on openings, but they reported that almost all trees were individuals or in clumps of 2 to 4 trees. Clyatt et al. (2016) examined historical forest structure in dry mixed-conifer stands in Montana, USA. They found that a large proportion of their stands were in openings, but little of the area was in core gaps. No clump size dominated in their study area. Clyatt et al. (2016) observed that the differences among these forests are likely driven by the overall stem densities, which in turn are driven by differences in productivity and fire frequency. As a result, while tree clump and opening patterns are a characteristic forest pattern following low- and moderate-severity fires, regional differences in the expression of those patterns are to be expected.

4.4. Control and reference areas versus First-entry fire areas

The similarity of opening and TAO clump patterns between the two first-entry fires and between reference areas despite the elevational differences suggests fires produce similar clump and opening structures despite differing management histories and elevation-associated differences in climate and topography and associated differences in productivity and forest structure (North et al., 2009).

We found that the two control areas had substantially different distributions of structure. The Big Meadow Fire control area met our expectation of an area that had not had a fire since 1878. It had a smaller proportion of area in openings and small clumps than its associated first-entry low-severity burn (Fig. 5). The pattern was reversed for the ARC Fires' control area and associated first-entry low-severity burn area. The more open and smaller clump nature of the ARC Fires' control area relative to its low-severity burn area may reflect both the greater disparity of elevation between the two compared to the Big Meadow study area and the ARC Fires' control area placement around a ridge.

4.5. Implications for forest managers

Forest managers who want to create more fire-resilient stand structures in fire-suppressed forests can use our results in several ways. First, managers can have greater confidence that wildfires allowed to burn under less-than-extreme weather conditions will produce clumping structures similar to historical and current reference opening and tree clump patterns (Jeronimo et al., 2019). Second, managers using prescribed fire to create tree clump and opening patterns may want to burn under conditions that could allow for burning with low to moderate severity since this produces patterns that best resemble our reference conditions and historical conditions (Collins et al., 2018; Lydersen et al., 2013). And third, managers using mechanical thinning to create resilient patterns can use the distribution of tree clump and opening structure classes identified in our study as a guide (Figs. 2 and 3).

For restoration activities using mechanical thinning, we believe that our tree clump and opening structure classes are better guides for restoration than using mean clump sizes as previous studies have recommended (e.g., Churchill et al., 2017) or the mean trends we also report in our study (Fig. 4). Both mean trends in clump sizes and the distributions of clump structure classes report similar general trends: smaller clumps and individuals become more common and the area in openings increases with increasing burn severity. However, the clump structure classes emphasize the heterogeneity of structures present following low- and moderate-severity burns. At the local scale (our 90 m^2 grid cells), while one clump size may be dominant, clumps of other sizes are also present (Fig. 2). The small clump class, as an example, which is a common structure associated with both low- and moderate-severity burns (Fig. 5), is characterized by a diversity of clump sizes at the local scale. At larger scales, managers may want to produce a spatially dispersed mixture of tree clump and opening patterns corresponding to our medium and small structure classes, which were all common in reference areas and following single entry low- or moderate-severity fire (Fig. 5). The unifying theme to both these suggestions for mechanical treatments is that fire produces a range of structures whether examining the diversity of clump sizes and area in openings within a structure class, or the diversity of structure classes associated with a particular burn severity. This gives managers the ability to use actual forest structures resulting from fires as guides while working with on-the-ground variations in topography and existing variations in forest structure.

Declaration of Competing Interest

The authors declare that they have no known competing financial interests or personal relationships that could have appeared to influence the work reported in this paper.

Acknowledgements

We thank Liz van Wagtendonk for preparing the maps in Fig. 1. United States Department of Agriculture Forest Service grants 13-CS-I 1052007-055, 13-JV-11261989-076, 14-JV-11261989-078, 15-JV-11261989-072, 16-JV-11261922-100, and 17-JV-11261989-067 funded the development of methods and analysis of data for this study.

Appendix A

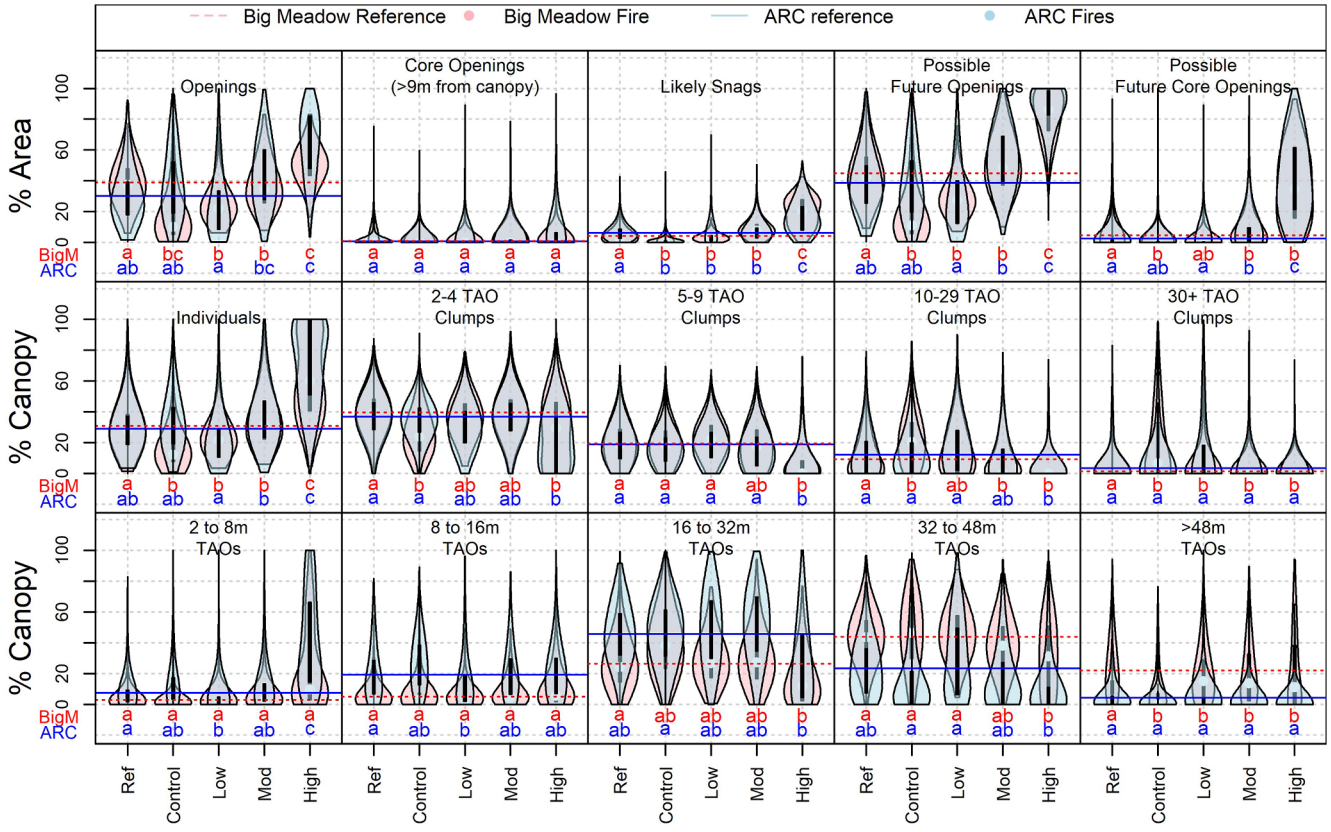

Fig. A1. This figure expands upon the information shown in Fig. 4. Area in openings, canopy area in different tree clump sizes (based on number of tree approximate objects (TAOs) per clump), and canopy area in different height strata of TAOs (lidar-identified overstory trees) among different classified burn severities and control areas relative to reference areas (horizontal lines). Open and core open areas shown both for current conditions and as potential future area by counting area currently classified as likely snags as potential future open areas. Pairwise distributions of all values are distinct at the equivalent of $p < 0.05$ using the Kolmogorov-Smirnov test. Letters below plots show differences in pairwise comparisons are based on niche overlap analysis with a < 80% overlap indicating a likely ecologically meaningful difference in distributions of values. Violin plots show the distribution of values within each height with lines showing the extent of the 25th to 75th percentile range and width showing the frequency of values. Percent area of openings and snags are relative to the total area of each 90 × 90 m grid cell, while percent area for tree clump and TAOs by height strata are relative to the total area in canopy > 2 m within each 90 × 90 m grid cell.

Appendix B. Supplementary material

Supplementary data to this article can be found online at https://doi.org/10.1016/j.foreco.2019.117659.

References

Abatzoglou, J.T., Williams, A.P., 2016. Impact of anthropogenic climate change on wildfire across western US forests. PNAS 113, 11770–11775. https://doi.org/10.1073/pnas.1607171113.

Agee, J.K., Skinner, C.N., 2005. Basic principles of forest fuel reduction treatments. For. Ecol. Manage. 211, 83–96.

Barth, M.A.F., Larson, A.J., Lutz, J.A., 2015. A forest reconstruction model to assess changes to Sierra Nevada mixed-conifer forest during the fire suppression era. For. Ecol. Manage. 354, 104–118. https://doi.org/10.1016/j.foreco.2015.06.030.

Bigelow, S.W., North, M.P., Salk, C.F., 2011. Using light to predict fuels-reduction and group-selection effects on succession in Sierran mixed-conifer forest. Can. J. For. Res. 41, 2051–2063. https://doi.org/10.1139/x11-120.

Bohlman, G.N., North, M., Safford, H.D., 2016. Shrub removal in reforested post-fire areas increases native plant species richness. For. Ecol. Manage. 374, 195–210. https://doi.org/10.1016/J.FORECO.2016.05.008.

Brodrick, P.G., Asner, G.P., 2017. Remotely sensed predictors of conifer tree mortality during severe drought. Environ. Res. Lett. 12, 115013. https://doi.org/10.1088/1748-9326/aa8f55.

Broennimann, O., Fitzpatrick, M.C., Pearman, P.B., Petitpierre, B., Pellissier, L., Yoccoz, N.G., Thuiller, W., Fortin, M.J., Randin, C., Zimmermann, N.E., Graham, C.H., Guisan, A., 2012. Measuring ecological niche overlap from occurrence and spatial environmental data. Glob. Ecol. Biogeogr. 21, 481–497. https://doi.org/10.1111/j.1466-8238.2011.00698.x.

Buchanan, J.B., Rogers, R.E., Pierce, D.J., Jacobson, J.E., 2003. Nest-site habitat use by white-headed woodpeckers in the eastern cascade mountains, Washington. Northwest. Nat. 84, 119–128. https://doi.org/10.2307/3536537.

Cansler, C.A., Swanson, M.E., Furniss, T.J., Larson, A.J., Lutz, J.A., 2019. Fuel dynamics after reintroduced fire in an old-growth Sierra Nevada mixed-conifer forest. Fire Ecol. 15, 16. https://doi.org/10.1186/s42408-019-0035-y.

Casas, Á., García, M., Siegel, R.B., Koltunov, A., Ramírez, C., Ustin, S., 2016. Burned forest characterization at single-tree level with airborne laser scanning for assessing wildlife habitat. Remote Sens. Environ. 175, 231–241. https://doi.org/10.1016/j.rse.2015.12.044.

Churchill, D.J., Carnwath, G.C., Larson, A.J., Jeronimo, S.M.A., 2017. Historical forest structure, composition, and spatial pattern in dry conifer forests of the western Blue Mountains, Oregon. In: General Technical Report PNW-GTR-956, Department of Agriculture. Forest Service, Pacific Northwest Research Station, pp. 93.

Churchill, D.J., Larson, A.J., Dahlgreen, M.C., Franklin, J.F., Hessburg, P.F., Lutz, J.A., 2013. Restoring forest resilience: from reference spatial patterns to silvicultural prescriptions and monitoring. For. Ecol. Manage. 291, 442–457. https://doi.org/10.1016/j.foreco.2012.11.007.

Clyatt, K.A., Crotteau, J.S., Schaedel, M.S., Wiggins, H.L., Kelley, H., Churchill, D.J., Larson, A.J., 2016. Historical spatial patterns and contemporary tree mortality in dry mixed-conifer forests. For. Ecol. Manage. 361, 23–37. https://doi.org/10.1016/j.

foreco.2015.10.049.
Collins, B.M., Fry, D.L., Lydersen, J.M., Everett, R., Stephens, S.L., 2017a. Impacts of different land management histories on forest change. Ecol. Appl. 27, 2475–2486. https://doi.org/10.1002/eap.1622.
Collins, B.M., Lydersen, J.M., Everett, R.G., Stephens, S.L., 2018. How does forest recovery following moderate-severity fire influence effects of subsequent wildfire in mixed-conifer forests? Fire Ecol. 14, 3. https://doi.org/10.1186/s42408-018-0004-x.
Collins, B.M., Roller, G.B., 2013. Early forest dynamics in stand-replacing fire patches in the northern Sierra Nevada, California. USA. Landsc. Ecol. 28, 1801–1813. https://doi.org/10.1007/s10980-013-9923-8.
Collins, B.M., Stevens, J.T., Miller, J.D., Stephens, S.L., Brown, P.M., North, M.P., 2017b. Alternative characterization of forest fire regimes: incorporating spatial patterns. Landsc. Ecol. 32, 1543–1552. https://doi.org/10.1007/s10980-017-0528-5.
Comfort, E.J., Clark, D.A., Anthony, R.G., Bailey, J., Betts, M.G., 2016. Quantifying edges as gradients at multiple scales improves habitat selection models for northern spotted owl. Landsc. Ecol. 31, 1227–1240. https://doi.org/10.1007/s10980-015-0330-1.
Coppoletta, M., Merriam, K.E., Collins, B.M., 2016. Post-fire vegetation and fuel development influences fire severity patterns in reburns. Ecol. Appl. 26, 686–699. https://doi.org/10.1890/15-0225.
Crockett, J.L., Westerling, A.L., Crockett, J.L., Westerling, A.L., 2018. Greater Temperature and Precipitation Extremes Intensify Western U.S. Droughts, Wildfire Severity, and Sierra Nevada Tree Mortality. J. Clim. 31, 341–354. https://doi.org/10.1175/JCLI-D-17-0254.1.
Daw, S.K., DeStefano, S., 2001. Forest characteristics of northern goshawk nest stands and post-fledging areas in oregon. J. Wildl. Manage. 65, 59. https://doi.org/10.2307/3803277.
Diffenbaugh, N.S., Swain, D.L., Touma, D., 2015. Anthropogenic warming has increased drought risk in California. PNAS 112, 3931–3936. https://doi.org/10.1073/pnas.1422385112.
Eidenshink, J., Schwind, B., Brewer, K., Zhu, Z., Quayle, B., Howard, S., 2007. A Project for monitoring trends in burn severity. Fire Ecol. 3 (1), 3–21. https://doi.org/10.4996/fireecology.0301003.
Fowells, H.A., Stark, N.B., 1965. Natural regeneration in relation to environment in the mixed conifer forest type of California. Res. Pap. PSW-RP-24. Berkeley, CA Pacific Southwest For. Range Exp. Station. For. Serv. U.S. Dep. Agric. 14, 24 p.
Franklin, J.F., Johnson, K.N., 2012. A Restoration Framework for Federal Forests in the Pacific Northwest. J. For. 110, 429–439. https://doi.org/10.5849/jof.10-006.
Fry, D.L., Stephens, S.L., Collins, B.M., North, M.P., Franco-Vizcaíno, E., 2014. Contrasting spatial patterns in active-fire and fire-suppressed mediterranean climate old-growth mixed conifer forests. PLoS One 9, e88985. https://doi.org/10.1371/journal.pone.0088985.
García, M., Saatchi, S., Casas, A., Koltunov, A., Ustin, S., Ramirez, C., Balzter, H., 2017. Extrapolating Forest Canopy Fuel Properties in the California Rim Fire by Combining Airborne LiDAR and Landsat OLI Data. Remote Sens. 9, 394. https://doi.org/10.3390/rs9040394.
Harrod, R.J., McRae, B.H., Hartl, W.E., 1999. Historical stand reconstruction in ponderosa pine forests to guide silvicultural prescriptions. For. Ecol. Manage. 114, 433–446. https://doi.org/10.1016/s0378-1127(98)00373-9.
Hollenbeck, J.P., Saab, V.A., Frenzel, R.W., 2011. Habitat suitability and nest survival of white-headed woodpeckers in unburned forests of Oregon. J. Wildl. Manage. 75, 1061–1071. https://doi.org/10.1002/jwmg.146.
Hood, S.M., Smith, S.L., Cluck, D.R., 2010. Predicting mortality for five California conifers following wildfire. For. Ecol. Manage. 260, 750–762.
Hu, T., Ma, Q., Su, Y., Battles, J.J., Collins, B.M., Stephens, S.L., Kelly, M., Guo, Q., 2019. A simple and integrated approach for fire severity assessment using bi- temporal airborne LiDAR data. Int. J. Appl. Earth Obs. Geoinf. 78, 25–38. https://doi.org/10.1016/j.jag.2019.01.007.
Jeronimo, S.M.A., 2018. Restoring Forest Resilience in the Sierra Nevada Mixed-Conifer Zone, with a Focus on Measuring Spatial Patterns of Trees using Airborne Lidar. PhD dissertation. University of Washington, Seattle, WA.
Jeronimo, S.M.A., Kane, V.R., Churchill, D.J., McGaughey, R.J., Franklin, J.F., 2018. Applying LiDAR individual tree detection to management of structurally diverse forest landscapes. J. For. 116, 336–346.
Jeronimo, S.M.A., 2015. LiDAR Individual Tree Detection for Assessing Structurally Diverse Forest Landscapes. MS thesis. College of the Environment, University of Washington, Seattle, WA.
Jeronimo, S.M.A., Kane, V.R., Churchill, D.J., Lutz, J.A., North, M.P., Asner, G.P., Franklin, J.F., 2019. Forest structure and pattern vary by climate and landform across active-fire landscapes in the montane Sierra Nevada. For. Ecol. Manage. 437, 70–86. https://doi.org/10.1016/j.foreco.2019.01.033.
Jeronimo, S.M.A., Lutz, J.A., Kane, V.R., Larson, A.J., Franklin, J.F., in re-review. Burn weather and meso-scale fuel structure provide a top-down template for post-fire tree mortality. Landscape Ecol.
Kane, Van R., Bakker, J.D., McGaughey, R.J., Lutz, J.A., Gersonde, R.F., Franklin, J.F., 2010a. Examining conifer canopy structural complexity across forest ages and elevations with LiDAR data. Can. J. For. Res. 40, 774–787. https://doi.org/10.1139/X10-064.
Kane, Van R., Cansler, C.A., Povak, N.A., Kane, J.T., McGaughey, R.J., Lutz, J.A., Churchill, D.J., North, M.P., 2015a. Mixed severity fire effects within the Rim fire: relative importance of local climate, fire weather, topography, and forest structure. For. Ecol. Manage. 358, 62–79. https://doi.org/10.1016/j.foreco.2015.09.001.
Kane, V.R., Lutz, J.A., Roberts, S.L., Smith, D.F., McGaughey, R.J., Povak, N.A., Brooks, M.L., 2013. Landscape-scale effects of fire severity on mixed-conifer and red fir forest structure in Yosemite National Park. For. Ecol. Manage. 287, 17–31. https://doi.org/10.1016/j.foreco.2012.08.044.
Kane, V.R., Lutz, J.A., Alina Cansler, C., Povak, N.A., Churchill, D.J., Smith, D.F., Kane, J.T., North, M.P., 2015b. Water balance and topography predict fire and forest structure patterns. For. Ecol. Manage. 338, 1–13. https://doi.org/10.1016/j.foreco.2014.10.038.
Kane, Van R., McGaughey, R.J., Bakker, J.D., Gersonde, R.F., Lutz, J.A., Franklin, J.F., 2010b. Comparisons between field- and LiDAR-based measures of stand structural complexity. Can. J. For. Res. 40, 761–773. https://doi.org/10.1139/x10-024.
Kane, V.R., North, M.P., Lutz, J.A., Churchill, D.J., Roberts, S.L., Smith, D.F., McGaughey, R.J., Kane, J.T., Brooks, M.L., 2014. Assessing fire effects on forest spatial structure using a fusion of Landsat and airborne LiDAR data in Yosemite National Park. Remote Sens. Environ. 151, 89–101. https://doi.org/10.1016/j.rse.2013.07.041.
Kennedy, M.C., Johnson, M.C., 2014. Fuel treatment prescriptions alter spatial patterns of fire severity around the wildland–urban interface during the Wallow Fire, Arizona, USA. For. Ecol. Manage. 318, 122–132.
Key, C.H., Benson, N.C., 2006. Landscape assessment: ground measure of severity, the Composite Burn Index, and remote sensing of severity, the Normalized Burn Ratio. In: Lutes, D.C., Keane, R.E., Caratti, J.F., Key, C.H., Benson, N.C., Sutherland, S., Gangi, L.J. (Eds.), FIREMON: Fire Effects Monitoring and Inventory System. Gen. Tech. Rep. RMRS-GTR-164-CD. Rocky Mountain Research Station, Fort Collins, Colorado, USA, pp. 1–51.
Knapp, E.E., Lydersen, J.M., North, M.P., Collins, B.M., 2017. Efficacy of variable density thinning and prescribed fire for restoring forest heterogeneity to mixed-conifer forest in the central Sierra Nevada, CA. For. Ecol. Manage. 406, 228–241. https://doi.org/10.1016/j.foreco.2017.08.028.
Lalonde, S.J., Mach, K.J., Anderson, C.M., Francis, E.J., Sanchez, D.L., Stanton, C.Y., Turner, P.A., Field, C.B., 2018. Forest management in the Sierra Nevada provides limited carbon storage potential: an expert elicitation. Ecosphere 9, e02321. https://doi.org/10.1002/ecs2.2321.
Larson, A.J., Churchill, D., 2012. Tree spatial patterns in fire-frequent forests of western North America, including mechanisms of pattern formation and implications for designing fuel reduction and restoration treatments. For. Ecol. Manage. 267, 74–92. https://doi.org/10.1016/j.foreco.2011.11.038.
Liang, S., Hurteau, M.D., Westerling, A.L., 2018. Large-scale restoration increases carbon stability under projected climate and wildfire regimes. Front. Ecol. Environ. 16, 207–212. https://doi.org/10.1002/fee.1791.
Lilliefors, H.W., 1969. On the Kolmogorov-Smirnov test for the exponential distribution with mean unknown. J. Am. Stat. Assoc. 64, 387–389. https://doi.org/10.1080/01621459.1969.10500983.
Lilliefors, H.W., 1967. On the Kolmogorov-Smirnov test for normality with mean and variance unknown. J. Am. Stat. Assoc. 62, 399–402. https://doi.org/10.1080/01621459.1967.10482916.
Lindenmayer, D.B., Laurance, W.F., Franklin, J.F., 2012. Global decline in large old trees. Science 338, 1305–1306. https://doi.org/10.1126/science.1231070.
Linn, R.R., Sieg, C.H., Hoffman, C.M., Winterkamp, J.L., McMillin, J.D., 2013. Modeling wind fields and fire propagation following bark beetle outbreaks in spatially-heterogeneous pinyon-juniper woodland fuel complexes. Agric. For. Meteorol. 173, 139–153. https://doi.org/10.1016/J.AGRFORMET.2012.11.007.
Lutz, J.A., Larson, A.J., Swanson, M.E., Freund, J.A., 2012. Ecological importance of large-diameter trees in a temperate mixed-conifer forest. PLoS One 7. https://doi.org/10.1371/journal.pone.0036131.
Lutz, J.A., Wagtendonk, J.W. Van, Franklin, J.F., 2009. Forest Ecology and Management Twentieth-century decline of large-diameter trees in Yosemite National Park, California, USA 257, 2296–2307. https://doi.org/10.1016/j.foreco.2009.03.009.
Lydersen, J.M., Collins, B.M., Miller, J.D., Fry, D.L., Stephens, S.L., 2016. Relating fire-caused change in forest structure to remotely sensed estimates of fire severity. Fire Ecol. 12, 99–116. https://doi.org/10.4996/fireecology.1203099.
Lydersen, J.M., North, M.P., Knapp, E.E., Collins, B.M., 2013. Quantifying spatial patterns of tree groups and gaps in mixed-conifer forests: reference conditions and long-term changes following fire suppression and logging. For. Ecol. Manage. 304, 370–382. https://doi.org/10.1016/j.foreco.2013.05.023.
Mallek, C.M., Safford, H., Viers, J., Miller, J., 2013. Modern departures in fire severity and area vary by forest type, Sierra Nevada and southern Cascades, California, USA. Ecosphere 4, 1–28. https://doi.org/10.1890/ES13-00217.
McCune, B., Grace, J.B., 2002. Analysis of Ecological Communities. MjM Software Design, Gleneden Beach, OR.
McDonald, P.M., Fiddler, G.O., 1989. Competing vegetation in ponderosa pine plantations: ecology and control. In: Gen. Tech. Rep. PSW-113. Pacific Southwest Research Station, Forest Service, U.S. Department of Agriculture, Berkeley, Calif., pp. 26. https://doi.org/10.2737/PSW-GTR-113.
McGaughey, R.J., 2018. FUSION/LDV: Software for LIDAR Data Analysis and Visualization: Version 3.70. USDA Forest Service Pacific Northwest Research Station, Seattle, WA. http://forsys.cfr.washington.edu/FUSION/fusion_overview.html.
McIntyre, P.J., Thorne, J.H., Dolanc, C.R., Flint, A.L., Flint, L.E., Kelly, M., Ackerly, D.D., 2014. Twentieth-century shifts in forest structure in California : denser forests, smaller trees, and increased dominance of oaks. PNAS 112, 1458–1463. https://doi.org/10.1073/pnas.1410186112.
Miller, C., Urban, D.L., 2000. Modeling the effects of fire management alternatives on Sierra Nevada mixed-conifer forests. Ecol. Appl. 10, 85–94.
Miller, J.D., Knapp, E.E., Key, C.H., Skinner, C.N., Isbell, C.J., Creasy, R.M., Sherlock, J.W., 2009. Calibration and validation of the relative differenced Normalized Burn Ratio (RdNBR) to three measures of fire severity in the Sierra Nevada and Klamath Mountains, California, USA. Remote Sens. Environ. 113, 645–656. https://doi.org/10.1016/j.rse.2008.11.009.
Miller, J.D., Skinner, C.N., Safford, H.D., Knapp, E.E., Ramirez, C.M., 2012. Trends and causes of severity, size, and number of fires in northwestern California, USA. Ecol. Appl. 22, 184–203.
Miller, J.D., Thode, A.E., 2007. Quantifying burn severity in a heterogeneous landscape

with a relative version of the delta Normalized Burn Ratio (dNBR). Remote Sens. Environ. 109, 66–80. https://doi.org/10.1016/j.rse.2006.12.006.
Mouillot, D., Stubbs, W., Faure, M., Dumay, O., Tomasini, J.A., Wilson, J.B., Chi, T. Do, 2005. Niche overlap estimates based on quantitative functional traits: a new family of non-parametric indices. Oecologia 145, 345–353. https://doi.org/10.1007/s00442-005-0151-z.
National Park Service, 2009. Big Meadow Prescribed Fire Review. URL https://www.nps.gov/yose/learn/management/upload/bigmeadowfirereport.pdf. (Accessed 6.9.19).
North, M., Collins, B.M., Stephens, S., 2012. Using Fire to Increase the Scale, Benefits, and Future Maintenance of Fuels Treatments. J. For. 110, 392–401. https://doi.org/10.5849/jof.12-021.
North, M., Stine, P., O'Hara, K., Zielinski, W., Stephens, S., 2009. An ecosystem management strategy for Sierran mixed-conifer forests. In: Gen. Tech. Rep. PSW-GTR-220 (Second printing, with addendum). U.S. Department of Agriculture Forest Service, Pacific Southwest Research Station, Albany, CA, pp. 49. https://doi.org/10.2737/PSW-GTR-220.
North, M.P., Kane, J.T., Kane, V.R., Asner, G.P., Berigan, W., Churchill, D.J., Conway, S., Gutiérrez, R.J., Jeronimo, S., Keane, J., Koltunov, A., Mark, T., Moskal, M., Munton, T., Peery, Z., Ramirez, C., Sollmann, R., White, A., Whitmore, S., 2017. Cover of tall trees best predicts California spotted owl habitat. For. Ecol. Manage. 405, 166–178. https://doi.org/10.1016/J.FORECO.2017.09.019.
North, M.P., Stevens, J.T., Greene, D.F., Coppoletta, M., Knapp, E.E., Latimer, A.M., Restaino, C.M., Tompkins, R.E., Welch, K.R., York, R.A., Young, D.J.N., Axelson, J.N., Buckley, T.N., Estes, B.L., Hager, R.N., Long, J.W., Meyer, M.D., Ostoja, S.M., Safford, H.D., Shive, K.L., Tubbesing, C.L., Vice, H., Walsh, D., Werner, C.M., Wyrsch, P., 2019. Tamm review: reforestation for resilience in dry western U.S. forests. For. Ecol. Manage. 432, 209–224. https://doi.org/10.1016/J.FORECO.2018.09.007.
Parsons, R., Linn, R., Pimont, F., Hoffman, C., Sauer, J., Winterkamp, J., Sieg, C., Jolly, W., Parsons, R.A., Linn, R.R., Pimont, F., Hoffman, C., Sauer, J., Winterkamp, J., Sieg, C.H., Jolly, W.M., 2017. Numerical investigation of aggregated fuel spatial pattern impacts on fire behavior. Land 6, 43. https://doi.org/10.3390/land6020043.
Paz-Kagan, T., Vaughn, N.R., Martin, R.E., Brodrick, P.G., Stephenson, N.L., Das, A.J., Nydick, K.R., Asner, G.P., 2018. Landscape-scale variation in canopy water content of giant sequoias during drought. For. Ecol. Manage. 419–420, 291–304. https://doi.org/10.1016/j.foreco.2017.11.018.
Pierce, K.B., Ohmann, J.L., Wimberly, M.C., Gregory, M.J., Fried, J.S., 2009. Mapping wildland fuels and forest structure for land management: a comparison of nearest neighbor imputation and other methods. Can. J. For. Res. 39, 1901–1916. https://doi.org/10.1139/X09-102.
Plotkin, J.B., Chave, J., Ashton, P.S., 2002. Cluster analysis of spatial patterns in Malaysian tree species. Am. Nat. 160, 629–644. https://doi.org/10.1086/342823.
R Core Team, 2013. R: A Language and Environment for Statistical Computing. R Foundation for Statistical Computing, Vienna, Austria.
Roberts, S.L., van Wagtendonk, J.W., Miles, A.K., Kelt, D.A., Lutz, J.A., 2008. Modeling the effects of fire severity and spatial complexity on small mammals in Yosemite National Park, California. Fire Ecol. 4, 83–104. https://doi.org/10.4996/fireecology.0402083.
Rothermel, R.C., 1991. Predicting behavior and size of crown fires in the Northern Rocky Mountains. In: Res. Pap. INT-438. US Department of Agriculture, Forest Service, Intermountain Research Station, Ogden, UT, pp. 438.
Safford, H.D., 2008. Fire Severity in Fuel Treatments American River Complex fire, Tahoe National Forest, California June 21 – August 1, 2008. URL http://www.sierraforestlegacy.org/Resources/Conservation/FireForestEcology/FireScienceResearch/FuelsManagement/FM-AmRivComplex8-2008.pdf.
Safford, H.D., Stevens, J.T., Merriam, K., Meyer, M.D., Latimer, A.M., 2012. Fuel treatment effectiveness in California yellow pine and mixed conifer forests. For. Ecol. Manage. 274, 17–28. https://doi.org/10.1016/J.FORECO.2012.02.013.
Sánchez Meador, A.J., Parysow, P.F., Moore, M.M., 2011. A New Method for Delineating Tree Patches and Assessing Spatial Reference Conditions of Ponderosa Pine Forests in Northern Arizona. Restor. Ecol. 19, 490–499. https://doi.org/10.1111/j.1526-100X.2010.00652.x.
Shive, K.L., Preisler, H.K., Welch, K.R., Safford, H.D., Butz, R.J., O'Hara, K.L., Stephens, S.L., 2018. From the stand scale to the landscape scale: predicting the spatial patterns of forest regeneration after disturbance. Ecol. Appl. 28, 1626–1639. https://doi.org/10.1002/eap.1756.
Skov, K.R., Kolb, T.E., Wallin, K.F., 2004. Tree Size and Drought Affect Ponderosa Pine Physiological Response to Thinning and Burning Treatments. For. Sci. 50, 81–91. https://doi.org/10.1093/forestscience/50.1.81.
Sollmann, R., White, A.M., Gardner, B., Manley, P.N., 2015. Investigating the effects of forest structure on the small mammal community in frequent-fire coniferous forests using capture-recapture models for stratified populations. Mamm. Biol. 80, 247–254. https://doi.org/10.1016/j.mambio.2015.03.002.
Sollmann, R., White, A.M., Tarbill, G.L., Manley, P.N., Knapp, E.E., 2016. Landscape heterogeneity compensates for fuel reduction treatment effects on Northern flying squirrel populations. For. Ecol. Manage. 373, 100–107. https://doi.org/10.1016/J.FORECO.2016.04.041.
Stephens, S.L., Collins, B.M., Biber, E., Fulé, P.Z., 2016. U.S. federal fire and forest policy : emphasizing resilience in dry forests 7, 1–19.
Stephens, S.L., Collins, B.M., Fettig, C.J., Finney, M.A., Hoffman, C.M., Knapp, E.E., North, M.P., Safford, H., Wayman, R.B., 2018. Drought, tree mortality, and wildfire in forests adapted to frequent fire. Bioscience 68, 77–88. https://doi.org/10.1093/biosci/bix146.
Stephens, S.L., Fry, D.L., Franco-Vizcaíno, E., 2008. Wildfire and spatial patterns in forests in northwestern Mexico: the United States wishes it had similar fire problems. Ecol. Soc. 13.
Stevens, J.T., Collins, B.M., Miller, J.D., North, M.P., Stephens, S.L., 2017. Changing spatial patterns of stand-replacing fire in California conifer forests. For. Ecol. Manage. 406, 28–36. https://doi.org/10.1016/J.FORECO.2017.08.051.
Symons, J.N., Fairbanks, D.H.K., Skinner, C.N., 2008. Influences of stand structure and fuel treatments on wildfire severity at Blacks Mountain Experimental Forest, northeastern California. Calif. Geogr. 48, 1–23.
Tuten, M.C., Sánchez Meador, A., Fulé, P.Z., 2015. Ecological restoration and fine-scale forest structure regulation in southwestern ponderosa pine forests. For. Ecol. Manage. 348, 57–67. https://doi.org/10.1016/j.foreco.2015.03.032.
Vaillant, N.M., Reinhardt, E.D., 2017. An evaluation of the forest service hazardous fuels treatment program—Are we treating enough to promote resiliency or reduce hazard? J. For. 115, 300–308. https://doi.org/10.5849/jof.16-067.
van Wagtendonk, J.W., Moore, P.E., 2010. Fuel deposition rates of montane and subalpine conifers in the central Sierra Nevada, California, USA. For. Ecol. Manage. 259, 2122–2132. https://doi.org/10.1016/j.foreco.2010.02.024.
Vincent, L., Soille, P., 1991. Watersheds in digital spaces – an efficient algorithm based on immersion simulations. IEEE Trans. Pattern Anal. Mach. Intell. 13, 583–598.
Walker, B., Holling, C.S., Carpenter, S., Kinzig, A., 2004. Resilience, adaptability and transformability in social–ecological systems. Ecol. Soc. 9 (2), 5. URL: http://www.ecologyandsociety.org/vol9/iss2/art5/.
Weatherspoon, C.P., Skinner, C.N., 1996. Landscape-level strategies for forest fuel management. In: Sierra Nevada Ecosystem Project: Final Report to Congress, Vol II. Assessments and Scientific Basis for Management Options. II University of California Center for Water and Wildland Resources, Davis, California.
Welch, K.R., Safford, H.D., Young, T.P., 2016. Predicting conifer establishment post wildfire in mixed conifer forests of the North American Mediterranean-climate zone. Ecosphere 7 (12), e01609. https://doi.org/10.1002/ecs2.1609.
Wiggins, H.L., Nelson, C.R., Larson, A.J., Safford, H.D., 2019. Using LiDAR to develop high-resolution reference models of forest structure and spatial pattern. For. Ecol. Manage. 434, 318–330. https://doi.org/10.1016/j.foreco.2018.12.012.
Wing, B.M., Ritchie, M.W., Boston, K., Cohen, W.B., Olsen, M.J., 2015. Individual snag detection using neighborhood attribute filtered airborne lidar data. Remote Sens. Environ. 163, 165–179. https://doi.org/10.1016/j.rse.2015.03.013.
Young, D.J.N., Stevens, J.T., Earles, J.M., Moore, J., Ellis, A., Jirka, A.L., Latimer, A.M., 2017. Long-term climate and competition explain forest mortality patterns under extreme drought. Ecol. Lett. 20, 78–86. https://doi.org/10.1111/ele.12711.
Ziegler, J.P., Hoffman, C., Battaglia, M., Mell, W., Paul, J., Hoffman, C., Battaglia, M., Mell, W., 2017. Spatially explicit measurements of forest structure and fire behavior following restoration treatments in dry forests. For. Ecol. Manage. 386, 1–12. https://doi.org/10.1016/j.foreco.2016.12.002.